

# Low Thresholds in Polymer Lasers on Conductive Substrates by Distributed Feedback Nanoimprinting: Progress Toward Electrically Pumped Plastic Lasers

By Ebinazar B. Namdas,\* Minghong Tong, Peter Ledochowitsch, Sarah R. Mednick, Jonathan D. Yuen, Daniel Moses, and Alan J. Heeger\*

Organic light-emitting materials are attractive for applications in organic light-emitting diodes (OLEDs), light-emitting field-effect transistors (LEFETs),<sup>[1–5]</sup> and as the gain medium in optically pumped lasers.<sup>[6–12]</sup> Lasing over the full range of the visible spectrum has been demonstrated using a number of semiconducting polymers with different molecular structures. Despite success in optically pumped lasing, the electrically pumped ‘polymer injection laser’ remains a significant challenge.<sup>[11]</sup> Three major obstacles must be overcome in order to demonstrate an electrically pumped laser:<sup>[13–16]</sup> i) the threshold for lasing must be decreased using an architecture containing the electrodes required for charge injection; ii) high carrier injection and high current densities must be demonstrated in the same device architecture; and iii) optical losses from charge-induced absorption must be reduced or eliminated.

Although the standard OLED configuration has been proposed, the losses in the two metal electrodes overcome the potential gain in the organic semiconductor. In order to reduce the optical loss in the OLED structure, one strategy is to increase the thickness of the organic layers to reduce the losses from the metal electrode. Kozlov et al.<sup>[17]</sup> showed that a 1.0  $\mu\text{m}$  thick organic layer could yield reasonable loss. Gartner et al. proposed an OLED structure as thick as 1.3  $\mu\text{m}$ .<sup>[18]</sup> However, because of the low carrier mobility in organic semiconductors, the thickness of the diode structure cannot be increased arbitrarily.

Recently, we reported very high current densities in the accumulation zone ( $\sim 2.5 \text{ kA cm}^{-2}$ ) in a LEFET device fabricated with a bilayer film comprising a hole-transport polymer, (poly 2,5-bis(3-tetradecylthiophen-2-yl) thiopheno[3,2-b]thiophene)-C14) and a light-emitting polymer, Super Yellow (SY), a poly(phenylene vinylene) derivative (see Figure 1 for structure).<sup>[19]</sup> Takenobu et al.<sup>[20]</sup> have also reported high current densities ( $\sim 4 \text{ kA cm}^{-2}$ ) in single-crystal LEFETs. Furthermore, in a LEFET configuration the position of the light-emitting zone can be controlled and placed well away from the source and drain electrodes. Because of these features, the LEFET structure offers specific advantages compared

to the conventional OLED structure as regards the fabrication of an injection laser.

Here, we show that a LEFET architecture with a distributed feedback (DFB) resonator structure nanoimprinted into the gain medium offers a route to achieving an electrically pumped plastic laser. We report here the results of a study of optically pumped lasing in a ‘Super Yellow’ film cast onto a gate dielectric and gate conducting (ITO) electrode, mimicking losses from the LEFET architecture. We apply nanoimprint lithography to fabricate 1D and 2D DFB grating resonator structures in multilayer films consisting of SY on  $\sim 200 \text{ nm}$  thick poly(vinyl alcohol) (PVA, serving as the gate dielectric) on quartz or ITO/glass substrates. The DFB structure was also fabricated on a doped silicon wafer substrate with bilayer dielectrics consisting of 200 nm thick PVA and 400 nm thick silicon nitride films. Lasing output intensity was measured under optical pumping using a Ti:sapphire laser at an excitation wavelength of  $\sim 400 \text{ nm}$ . We demonstrate that the 2D DFB laser provides a lower lasing threshold than the 1D DFB laser under identical conditions. The nanoimprinted 2D DFB

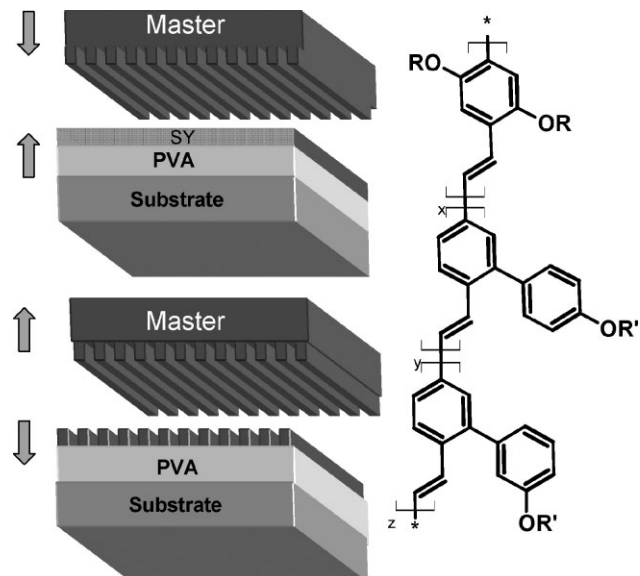


**Figure 1.** Schematic fabrication steps for the DFB structure. A rigid nanostructure template, a ‘master,’ is pressed at 400 psi onto the polymer film and heated to 140 °C for 120 s. Upon heating, the polymer becomes fluid and fills the empty space of the master, forming a nanopattern which is a negative of the master. Finally, the sample is carefully separated from the master. A molecular structure of Super Yellow is shown in the side panel.

[\*] Dr. E. B. Namdas, Prof. A. J. Heeger, Dr. M. Tong, P. Ledochowitsch, S. R. Mednick, J. D. Yuen, Dr. D. Moses  
Center for Polymers and Organic Solids, University of California Santa Barbara, CA 93106 (USA)  
E-mail: ebnamdas@ipos.ucsb.edu; ajhe@physics.ucsb.edu

DOI: 10.1002/adma.200802436

lasers exhibit excellent characteristics with a lasing threshold and slope efficiency of 32 nJ/pulse and 1.2%, respectively.

Hot-embossing, a recently developed nanoimprint lithography (NIL) method, is capable of low-cost, high-throughput, large-area nanopatterning of thermoplastic thin films.<sup>[21–24]</sup> A rigid nanostructure template, a ‘master,’ is pressed onto the polymer film and heated to above the glass-transition temperature ( $T_g$ ). Upon heating, the polymer becomes fluid and fills the empty spaces in the master, forming a nanopattern that is a negative of the pattern on the master. Finally, the sample is carefully separated from the master.

Figure 1 shows the molecular structure of SY and the DFB laser architecture. Samples were prepared on quartz, ITO, and Si wafer substrates as follows: 1) SY/PVA/quartz; 2) SY/PVA/ITO; and 3) SY/PVA on 400 nm thick silicon nitride on n<sup>++</sup> silicon (SY/PVA/SiNx/Si). PVA was spin-cast first from solution (5% PVA in DI (deionized) water). The SY (0.6 wt % in toluene), was then spin-cast onto the PVA film at 1000 rpm to serve as the lasing material. The thicknesses of the PVA and SY films were ~200 nm and ~100 nm, respectively. The SY films were hot-embossed in a commercial nanoimprinter (Nanonex NX 2000). The imprinting was carried out at 140 °C and 400 psi (1 psi = 6.894 kPa) pressure for 120 s.

Figure 2a and b shows high-resolution scanning electron microscopy (SEM) images of the master. The 1D grating consists of arrays of lines with a periodicity of 344 nm; the 2D grating consists of a square array of pillars with a 344 nm period. Cross sectional SEM images showed 100 nm feature definition for both the 1D and 2D gratings. Figure 2c and d show high-resolution SEM images of the imprinted 1D and 2D gratings on an SY/PVA/ITO sample. The 344 nm periodicity for both the 1D and the 2D master are faithfully replicated on the samples. The depth of the printed samples was about ~30 nm, as determined by atomic force microscopy (AFM). The polymer shrinks around the

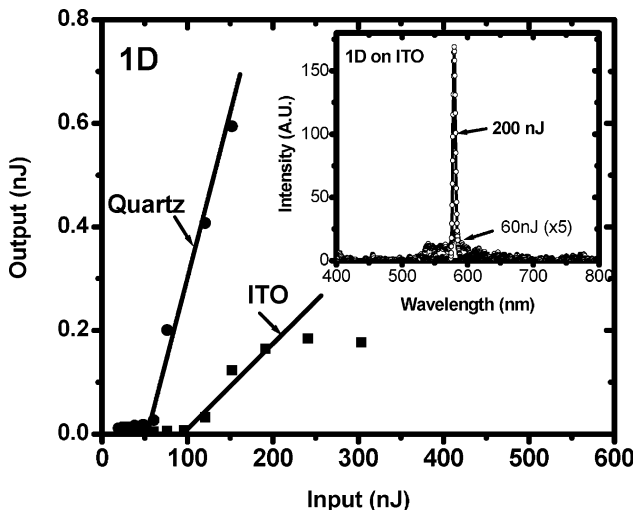


**Figure 3.** Output energy as a function of pump energy for 1D DFB on SY/PVA/quartz and SY/PVA/ITO substrates. The inset shows laser spectra below and above the lasing threshold.

stamped pillar array during cooling resulting in a round shaped ‘hole’ feature.

Figure 3 shows the emission output of the 1D DFB laser on the SY/PVA/quartz and SY/PVA/ITO samples as a function of excitation pump energy. On both substrates, we observed a lasing threshold as indicated by an abrupt change in the slope of the output energy, followed by a linear increase in output signal as the pump energy increased beyond the threshold. For pump excitation below threshold, the spectra are broad and featureless, whereas for pump excitation above the lasing threshold, a narrow peak arose at 580 nm with full width at half maximum of <3 nm.

The measured spectral width was limited by the resolution of spectrometer.

From the Bragg expression,  $m\lambda_m = 2n_{\text{eff}} \Lambda$ , where  $\Lambda$  is the periodicity of the grating,  $m$  is the order of the diffraction, and  $n_{\text{eff}}$  is the effective refractive index of the waveguide. Considering  $n_{\text{eff}} \sim 1.7$ , we obtained second-order diffraction from the DFB grating. The lowest threshold, 32 nJ/pulse, was obtained from the SY/PVA/quartz structure. For SY/PVA/ITO, the laser threshold increased to 100 nJ/pulse.

The slope efficiencies were calculated for the 1D DFB laser from the input/output energies. The slope efficiency was 0.65% and 0.2% for the SY/PVA/quartz and SY/PVA/ITO samples, respectively. The higher threshold and reduced slope efficiency for the ITO substrate indicates optical loss in the resonator. This optical loss is attributed to penetration of the lasing modes into the conducting ITO electrode; the loss is significant even though the ITO electrode is separated from the SY by a 200 nm thick PVA dielectric.

Figure 4 shows the output emission characteristics of 2D DFB lasers on SY/PVA/quartz and SY/PVA/ITO as a function of excitation

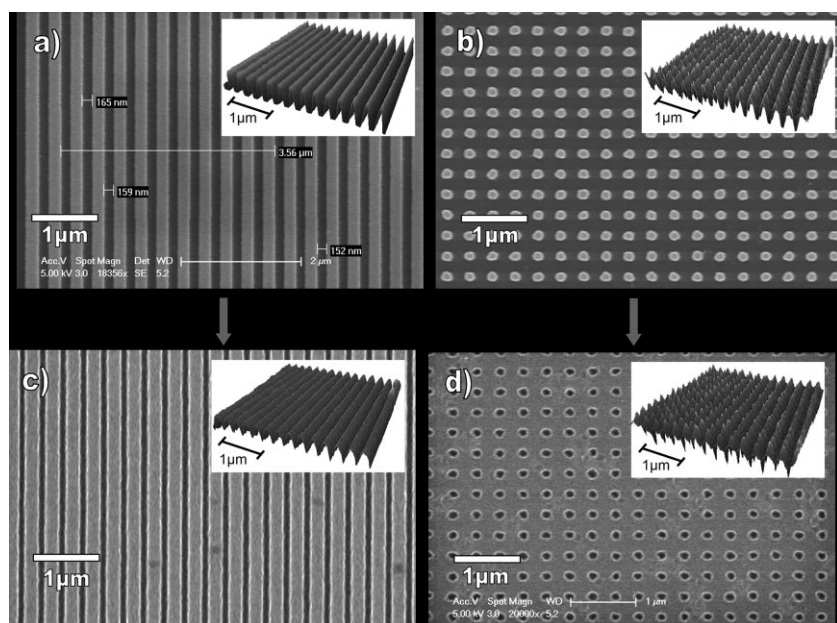


**Figure 2.** SEM and AFM images (inset) of a) the 1D master, b) the 2D master, c) the nanoimprinted 1D DFB structure on SY/PVA/ITO, and d) the nanoimprinted 2D DFB structure on SY/PVA/ITO.

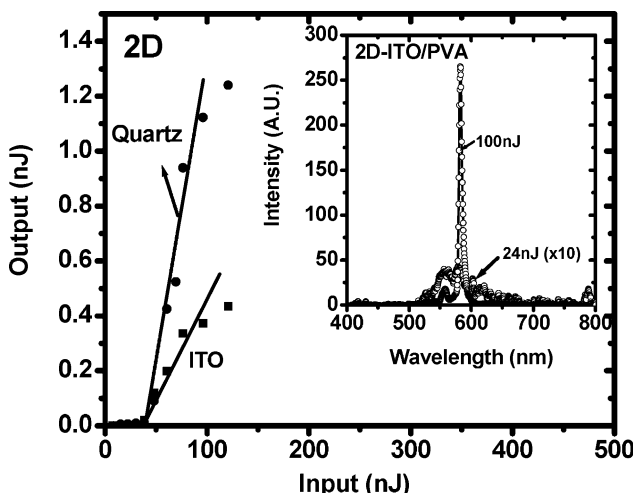


**Figure 4.** Output energy as a function of pump energy for 2D DFB on SY/PVA/quartz and SY/PVA/ITO substrates. The inset shows the laser below and above the lasing threshold.

pump energy. Both structures exhibited lasing thresholds of approximately 35 nJ/pulse. As expected for pump excitation below threshold, the spectrum was broad, whereas for pump excitation above the threshold for lasing, a narrow peak emerged at 582 nm. The slope efficiencies from input/output characteristics were 1.2% and 0.65% for the SY/PVA/Quartz and SY/PVA/ITO samples respectively. The data indicate that the lasing threshold for the 2D resonator on the ITO substrate drops significantly (by a factor of three), whereas the slope efficiency increases by a factor of three compared to the 1D resonator on the ITO substrate. To the best of our knowledge, this is the first report of a reduction in the lasing threshold using a 2D resonator fabricated on an ITO electrode. We attribute the lower threshold and the higher slope efficiency to better optical confinement resulting in increased feedback in the 2D resonator. Residual optical losses from the penetration and absorption of the lasing mode into the conducting ITO electrode are overcome by the increase in the feedback of the 2D resonator. These results indicate the potential utility of the 2D DFB resonator superposed onto the LEFET architecture, with ITO as the gate electrode.

We have also investigated the optical lasing threshold of SY on a silicon wafer substrate, the configuration routinely used for LEFETs. The  $n^{++}$  silicon wafer was first coated with a 400 nm thick silicon nitride layer by using plasma-enhanced chemical vapor deposition (PECVD) and then spin-coated with  $\sim$ 200 nm thick PVA; the total spacing between the SY and the conducting gate electrode was about 600 nm. When the 1D and 2D DFB imprinted samples were excited by the pump laser, lasing was not observed even at pump energies of up to 0.5 mJ/pulse, the maximum available pump intensity from the Ti:sapphire laser system. This indicates the dominance of the optical loss mechanisms in this structure. The optical loss results from substantial absorption by the silicon in the visible spectral range and the high refractive index of silicon, which prevents the confinement of the lasing mode in the resonator cavity. These findings imply that adequate device architecture is necessary for lasing with silicon substrate,<sup>[9]</sup> or, alternatively, ITO should be

used as the gate electrode in attempts to demonstrate LEFET lasers.

For the SY/PVA/quartz samples without the DFB grating, the onset of line narrowing through amplified spontaneous emission (ASE) was  $\sim$ 315 nJ/pulse. The sample without DFB grating was again excited at  $\sim$ 20° to the film normal, and the spectral output from the films was measured at close to normal incidence. These observations indicate that by using the DFB grating structure, we were able to lower the ASE lasing threshold by a factor of approximately ten.

From these measurements, we can estimate the lasing threshold required for electrically pumped lasers. We obtained the lowest lasing threshold for SY of 32 nJ/pulse. This corresponds to a photon density of  $7.2 \times 10^{12} \text{ cm}^{-2}$  (or  $3.6 \mu\text{J cm}^{-2}$ ) in the pump laser. Because only 25% of pump energy is absorbed by the SY film at 400 nm excitation, the density of excitation at the lasing threshold is approximately  $1.8 \times 10^{12} \text{ cm}^{-2}$ . Taking into account the photoluminescence quantum yield ( $\Phi_{pl}$ ) of the SY film,  $\sim$ 53%,<sup>[25]</sup> we estimate the density of emitted photons (generated by photoluminescence) near the lasing threshold as  $10^{12} \text{ cm}^{-2}$ . This is the minimum photon density necessary for lasing and must be generated electrically (by electroluminescence) to reach the threshold for electrically pumped laser. Assuming that there are no other optical losses, e.g., from carrier-induced absorption, then the lasing threshold for the injection current can be estimated by the following equation

$$J_{th} \approx \frac{No \times q}{\Phi_{int-el} \times \tau_{rad}} \quad (1)$$

where  $No$  is density of photons at the lasing threshold ( $1 \times 10^{12} \text{ cm}^{-2}$ ),  $q$  is electrical charge,  $\Phi_{int-el}$  is the internal quantum efficiency for the electroluminescence, and  $\tau_{rad}$  is the radiative lifetime of the excitons. The highest reported value of the external quantum efficiency of SY LEFETs is 0.5%,<sup>[4]</sup> implying an internal quantum efficiency of 2.5% (estimated assuming 80% of the photons are trapped by the dielectric mismatch<sup>[26]</sup> inside the light-emitting polymer and gate dielectrics). With  $\Phi_{int-el} \sim 2.5\%$ , and  $\tau_{rad}$  for SY  $\sim$ 5 ns,<sup>[27]</sup> we estimate the lasing threshold for the injection current to be  $\sim$ 1.2 kA  $\text{cm}^{-2}$ . This value has already been demonstrated ( $\sim$ 2.5 kA  $\text{cm}^{-2}$ ) for the current density in the LEFET,<sup>[19]</sup> calculated assuming carrier confinement takes place within a thickness of  $\sim$ 2 nm. Note, however, that although the injected carriers are confined to the accumulation layer near the interface with the gate dielectric, the excitons in the recombination zone can spread to the thickness of the luminescent polymer (100 nm). Thus,  $\sim$ 60 kA  $\text{cm}^{-2}$  is a realistic estimate of the threshold current density for lasing with the LEFET architecture.

In summary, we have demonstrated that 1D or 2D DFB gratings can be directly incorporated into the LEFET device structure by nanoimprint lithography. Both the 1D and 2D gratings have merits. Although the 2D grating yielded a lower threshold in these initial experiments, the 1D grating can provide a high degree of chain orientation for the organic semiconducting polymers in the source-drain channel.<sup>[28]</sup> The results presented

here open up a new opportunity for LEFET research using NIL. Although increasing the current density by a factor of 50 is a serious challenge, this challenge can be met by implementing a number of approaches including reducing the channel length, increasing the gate capacitance, using polymers with higher PL quantum efficiency, and by using pulsed operation to higher voltages. Moreover, as demonstrated earlier,<sup>[25]</sup> the losses that limit the gain can be further reduced by a factor of twenty-five using polymer blends and the Förster energy transfer mechanism. Our focus during the next period of this research will be to implement these improvements with the goal of successfully demonstrating the organic injection laser.

## Experimental

The master, consisting of 1D and 2D gratings, was fabricated by electron-beam (e-beam) lithography (JEOL FS-6300) on a fused 200 nm thick SiO<sub>2</sub> on silicon (500 μm) substrate. After cleaning the substrate, ZEP-520, a positive e-beam resist was spin-cast onto the master at 3000 rpm. Subsequently, a thin layer of conductive polyaniline was deposited in order to avoid charging of the nonconductive resist and SiO<sub>2</sub> during the e-beam write. After the e-beam exposure, the patterns were rinsed, developed, and etched. The period for both the 1D and 2D gratings was chosen to be  $\Lambda = 344$  nm, matching the second-order Bragg condition suitable for the emission wavelength of the SY. The 2D grating consisted of a square array of pillars with 344 nm period. Each grating covers an area of 3 mm × 3 mm; the 1D and 2D gratings were simultaneously fabricated on the same substrate for direct comparison.

The samples were mounted in a vacuum chamber and maintained under a pressure of  $\sim 10^{-6}$  mbar to avoid degradation of the SY by oxygen. The samples were optically pumped using a frequency-doubled Ti:sapphire laser, which produced 100 fs pulses at a wavelength of 400 nm with a repetition rate of 1 kHz. The output of the laser beam was attenuated using neutral density filters and then focused using a cylindrical lens to form a rectangular shape with a length of 2.5 mm and width of  $\sim 350$  μm. The pump beam was aligned at  $\sim 20^\circ$  to the film normal. The spectral output and the output energy from the films were measured in a direction close to normal incidence using an Ocean Optics fiber-coupled CCD (charge-coupled device) spectrograph (USB 2000) with a spectral resolution of approximately 3 nm. The sample emits two beams in opposite directions normal to the surface; the emitted pulse energies and slope efficiencies quoted in this article are the measured for a single beam.

## Acknowledgements

Support for research was provided by the Air Force Office of Scientific Research (Charles Lee, Program Officer) and by the National Science Foundation (Polymer program, NSF-DMR-0602280). The "Super Yellow" material was provided by Covion.

Received: August 20, 2008

Revised: October 30, 2008

Published online: December 12, 2008

- [1] R. H. Friend, R. W. Gymer, A. B. Holmes, J. H. Burroughes, R. N. Marks, C. Taliani, D. D. C. Bradley, D. A. Dos Santos, J. L. Bredas, M. Logdlund, W. R. Salaneck, *Nature* **1999**, 397, 121.
- [2] J. Zaumseil, R. H. Friend, H. Sirringhaus, *Nat. Mater.* **2006**, 5, 69.
- [3] J. S. Swensen, C. Soci, A. J. Heeger, *Appl. Phys. Lett.* **2005**, 87, 253511.
- [4] E. B. Namdas, J. S. Swensen, P. Ledochowitsch, J. D. Yuen, D. Moses, A. J. Heeger, *Adv. Mater.* **2008**, 20, 1321.
- [5] M. Muccini, *Nat. Mater.* **2006**, 5, 605.
- [6] F. Hide, M. A. DiazGarcia, B. J. Schwartz, M. R. Andersson, Q. B. Pei, A. J. Heeger, *Science* **1996**, 273, 1833.
- [7] T. Rabe, M. Hoping, D. Schneider, E. Becker, H. H. Johannes, W. Kowalsky, T. Weimann, J. Wang, P. Hinze, B. S. Nehls, U. Scherf, T. Farrell, T. Riedl, *Adv. Funct. Mater.* **2005**, 15, 1188.
- [8] P. Gorm, T. Rabe, T. Riedl, W. Kowalsky, F. Galbrecht, U. Scherf, *Appl. Phys. Lett.* **2006**, 89, 161113.
- [9] H. Nakanotani, S. Akiyama, D. Ohnishi, M. Moriwake, M. Yahiro, T. Yoshihara, S. Tobita, C. Adachi, *Adv. Funct. Mater.* **2007**, 17, 2328.
- [10] J. R. Lawrence, E. B. Namdas, G. J. Richards, P. L. Burn, I. D. W. Samuel, *Adv. Mater.* **2007**, 19, 3000.
- [11] a) I. D. W. Samuel, G. A. Turnbull, *Chem. Rev.* **2007**, 107, 1272. b) I. D. W. Samuel, *Nature* **2004**, 429, 709.
- [12] B. K. Yap, R. D. Xia, M. Campoy-Quiles, P. N. Stavrinou, D. D. C. Bradley, *Nat. Mater.* **2008**, 7, 376.
- [13] M. Reufer, S. Riechel, J. M. Lupton, J. Feldmann, U. Lemmer, D. Schneider, T. Benstem, T. Dobbertin, W. Kowalsky, A. Gombert, K. Forberich, V. Wittwer, U. Scherf, *Appl. Phys. Lett.* **2004**, 84, 3262.
- [14] P. Gorm, T. Rabe, T. Riedl, W. Kowalsky, *Appl. Phys. Lett.* **2007**, 91, 041113.
- [15] V. G. Kozlov, G. Parthasarathy, P. E. Burrows, V. B. Khalfin, J. Wang, S. Y. Chou, S. R. Forrest, *IEEE J. Quantum Electron.* **2000**, 36, 18.
- [16] S. Lattante, F. Romano, A. P. Caricato, M. Martino, M. Anni, *Appl. Phys. Lett.* **2006**, 89, 031108.
- [17] V. G. Kozlov, V. Bulovic, P. E. Burrows, S. R. Forrest, *Nature* **1997**, 389, 362.
- [18] C. Gartner, C. Karnutsch, U. Lemmer, C. Pfleum, *J. Appl. Phys.* **2007**, 101, 023107.
- [19] E. B. Namdas, P. Ledochowitsch, J. D. Yuen, D. Moses, A. J. Heeger, *Appl. Phys. Lett.* **2008**, 92, 183304.
- [20] T. Takenobu, S. R. Bisri, T. Takahashi, M. Yahiro, C. Adachi, Y. Iwasa, *Phys. Rev. Lett.* **2008**, 100, 066601.
- [21] S. Y. Chou, P. R. Krauss, P. J. Renstrom, *Appl. Phys. Lett.* **1995**, 67, 3114.
- [22] Y. Chen, Z. Li, Z. Zhang, D. Psaltis, A. Scherer, *Appl. Phys. Lett.* **2007**, 91, 051109.
- [23] E. Mele, A. Camposeo, R. Stabile, P. Del Carro, F. Di Benedetto, L. Persano, R. Cingolani, D. Pisignano, *Appl. Phys. Lett.* **2006**, 89, 131109.
- [24] V. Reboud, P. Lovera, N. Kehagias, M. Zelmann, C. Schuster, F. Reuther, G. Gruetzner, G. Redmond, C. M. S. Torres, *Appl. Phys. Lett.* **2007**, 91, 151101.
- [25] R. Gupta, M. Stevenson, A. J. Heeger, *J. Appl. Phys.* **2002**, 92, 4874.
- [26] C. Adachi, M. A. Baldo, M. E. Thompson, S. R. Forrest, *J. Appl. Phys.* **2001**, 90, 5048.
- [27] H. Najafov, I. Biaggio, T. K. Chuang, M. K. Hatalis, *Phys. Rev. B* **2006**, 73, 125202.
- [28] Z. J. Hu, B. Muls, L. Gence, D. A. Serban, J. Hofkens, S. Melinte, B. Nysten, S. Demoustier-Champagne, A. M. Jonas, *Nano Lett.* **2007**, 7, 3639.